B-FLOWS: Biofouling Focused Learning and Observation for Wide-Area Surveillance in Tidal Stream Turbines

Haroon Rashid, Houssem Habbouche, Yassine Amirat, Abdeslam Mamoune, Hosna Titah-Benbouzid, Mohamed Benbouzid

Journal of *Marine Science and Engineering*

MDPI

Article

B-FLOWS: Biofouling Focused Learning and Observation for Wide-Area Surveillance in Tidal Stream Turbines

Haroon Rashid [1], Houssem Habbouche [2], Yassine Amirat [3], Abdeslam Mamoune [1], Hosna Titah-Benbouzid [1] and Mohamed Benbouzid [1,*]

[1] Institut de Recherche Dupuy de Lôme (UMR CNRS 6027), University of Brest, 29238 Brest, France; haroon.rashid@univ-brest.fr (H.R.); abdeslam.mamoune@univ-brest.fr (A.M.); hosna.titahbenbouzid@gmail.com (H.T.-B.)
[2] Ecole Militaire Polytechnique, Mechanical Structures Laboratory, Algiers 16046, Algeria; houssem.habbouche@emp.mdn.dz
[3] ISEN Yncréa Ouest, L@bISEN, 29200 Brest, France; yassine.amirat@isen-ouest.yncrea.fr
* Correspondence: mohamed.benbouzid@univ-brest.fr

Abstract: Biofouling, the accumulation of marine organisms on submerged surfaces, presents significant operational challenges across various marine industries. Traditional detection methods are labor intensive and costly, necessitating the development of automated systems for efficient monitoring. The study presented in this paper focuses on detecting biofouling on tidal stream turbine blades using camera-based monitoring. The process begins with dividing the video into a series of images, which are then annotated to identify and select the bounding boxes containing objects to be detected. These annotated images are used to train YOLO version 8 to detect biofouled and clean blades in the images. The proposed approach is evaluated using metrics that demonstrate the superiority of this YOLO version compared to previous ones. To address the issue of misdetection, a data augmentation approach is proposed and tested across different YOLO versions, showing its effectiveness in improving detection quality and robustness.

Keywords: tidal stream turbine; biofouling; detection; YOLO; data augmentation

Citation: Rashid, H.; Habbouche, H.; Amirat, Y.; Mamoune, A.; Titah-Benbouzid, H.; Benbouzid, M. B-FLOWS: Biofouling Focused Learning and Observation for Wide-Area Surveillance in Tidal Stream Turbines. *J. Mar. Sci. Eng.* **2024**, *12*, 1828. https://doi.org/10.3390/jmse12101828

Academic Editor: Francesca Cima

Received: 18 August 2024
Revised: 4 October 2024
Accepted: 9 October 2024
Published: 13 October 2024

1. Introduction

As the demand for renewable energy sources continues to rise, tidal stream turbines (TSTs) have emerged as a promising technology for harnessing the immense power of ocean currents. However, one of the significant challenges facing the operational efficiency of these turbines is biofouling—the accumulation of marine organisms such as algae, barnacles, and mollusks on submerged surfaces. Biofouling not only increases drag and reduces the hydrodynamic efficiency of the turbine blades but also accelerates material degradation and necessitates frequent maintenance, leading to increased operational costs and downtime [1]. Beyond the mechanical and operational challenges, biofouling also poses a significant risk to the long-term durability of tidal energy infrastructure [2]. The accumulation of marine organisms can cause corrosion and damage protective coatings, weakening structural components. Over time, this can lead to more frequent replacements of parts such as blades and nacelles, reducing the overall lifespan of the turbine. Additionally, biofouling-induced vibrations can disrupt the dynamic balance of rotating components, amplifying fatigue stress on mechanical parts. This increases maintenance demands and raises safety concerns, particularly for large-scale tidal installations deployed in remote or harsh marine environments [3].

The impact of biofouling on TSTs can be substantial, as illustrated in Figure 1 [4], which shows the stark contrast between a clean turbine and the one affected by biofouling. The accumulation of marine organisms on the turbine's surfaces, as seen in the Sabella TST

case, highlights the critical need for effective monitoring and maintenance strategies to mitigate these effects.

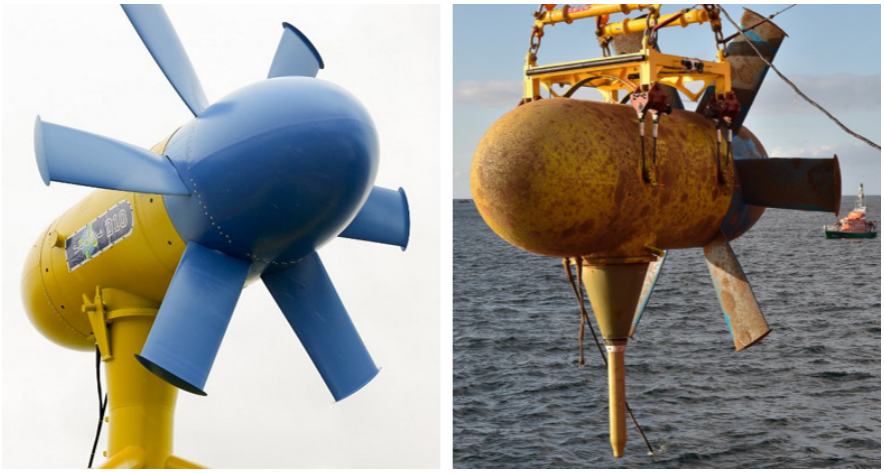

Figure 1. Biofouling accumulation on the Sabella tidal stream turbine. Reproduced from [4].

Figure 1 underscores the critical need for effective monitoring and maintenance strategies to mitigate these effects. The early detection of biofouling can enable timely interventions that prevent severe performance degradation, thus optimizing maintenance schedules and reducing operational costs. Furthermore, the implementation of advanced monitoring systems, such as real-time imaging and automated detection technologies, can facilitate proactive maintenance approaches, allowing operators to address biofouling issues before they escalate. As the deployment of tidal energy systems continues to expand, developing reliable and efficient biofouling monitoring solutions will be essential for ensuring the long-term viability and sustainability of this renewable energy technology.

To address this issue, it is crucial to develop effective biofouling detection systems that can operate in the challenging underwater environment, enabling timely interventions and maintenance. Traditional methods for biofouling detection often rely on manual inspection or complex imaging techniques, which can be time-consuming and resource-intensive [5]. Manual inspections may involve divers or remotely operated vehicles (ROVs), both are limited by human factors such as fatigue, visibility, and safety concerns. Additionally, complex imaging techniques, such as sonar or high-resolution cameras, can generate vast amounts of data that require extensive analysis, often leading to delayed responses in maintenance.

In recent years, machine learning algorithms have shown significant promise in automating the detection and classification of various underwater phenomena, including biofouling [6]. Among these, the YOLO (You Only Look Once) algorithm has gained widespread popularity due to its ability to perform real-time object detection with high accuracy and efficiency [7–9]. YOLO's architecture allows it to process images in a single pass, which is particularly advantageous for monitoring dynamic underwater environments where conditions can change rapidly. By leveraging YOLO and similar machine learning techniques, it becomes possible to create robust biofouling detection systems that not only enhance the accuracy of monitoring efforts but also facilitate proactive maintenance interventions, ultimately improving the operational efficiency of TSTs.

In this paper, we propose B-FLOWS, a lightweight and optimized adaptation of the YOLO algorithm, specifically designed for biofouling detection in TSTs. Our approach aims to combine the robust detection capabilities of YOLO with a streamlined architecture tailored to the unique requirements of underwater monitoring. B-FLOWS offers a practical solution for continuous biofouling monitoring in tidal energy systems by reducing the computational load and improving the real-time processing capability.

This work contributes to the growing body of research focused on enhancing marine renewable energy technologies' operational efficiency and sustainability. We evaluated the

performance of B-FLOWS through extensive testing on datasets collected from a real-world TST installation, demonstrating its effectiveness in detecting and classifying various forms of biofouling with high accuracy.

2. Related Works

The application of deep learning to biofouling detection is an emerging area of research. Previous studies have explored various image processing techniques and machine learning algorithms, but few have leveraged the capabilities of modern object detection frameworks like YOLO.

2.1. Advances in Object Detection Networks

Target detection has been one of the most significant advancements in computer vision, particularly with the rise of deep learning [10,11]. Early methods, such as the Viola–Jones detector, relied on handcrafted features and traditional machine learning techniques for object detection [12]. However, the advent of convolutional neural networks (CNNs) revolutionized the field by enabling automatic feature extraction and end-to-end learning, leading to substantial improvements in accuracy and efficiency.

The development of target detection networks has seen several milestones. The introduction of the R-CNN (Region-based Convolutional Neural Network) marked a significant breakthrough by combining region proposal methods with CNNs to improve object detection accuracy [13]. This was followed by the development of Fast R-CNN, Faster R-CNN, and Mask R-CNN, which further optimized the speed and accuracy by integrating region proposal networks directly into the detection pipeline [14].

Another major advancement was the development of single-stage detectors such as YOLO and SSD (Single-Shot MultiBox Detector) [15]. These algorithms prioritized speed by eliminating the need for region proposals, enabling real-time object detection. YOLO, in particular, gained popularity due to its simplicity and efficiency, making it an ideal choice for applications requiring rapid and accurate detection [16–20].

Recent developments have focused on improving the efficiency and accuracy of these networks through techniques like feature pyramid networks (FPNs), anchor-free detection, and transformer-based architectures [21]. Lightweight models such as MobileNet and Tiny YOLO have also been introduced to facilitate deployment on edge devices with limited computational resources, which is particularly relevant for real-time biofouling detection on TSTs.

2.2. Evolution of Biofouling Detection Techniques

Biofouling detection has evolved alongside maintenance policies, starting with corrective maintenance, where the generator was allowed to stop before cleaning could be considered. The approach then progressed to systematic preventive maintenance, in which a cleaning schedule was defined to prevent unexpected generator shutdowns. With the advent of condition-based maintenance and monitoring techniques, it became possible to schedule inspections to assess the generator's condition and plan cleaning without unexpected stops, optimizing its use. Among these monitoring techniques is video monitoring [22]. Unfortunately, the images obtained are generally noisy and require image processing techniques such as thresholding, edge detection and morphological operations [23,24]. However, these methods are often labor-intensive, time-consuming, and prone to inaccuracies due to the complex and dynamic nature of marine environments [25]. Maintenance further evolved toward intelligent maintenance, which aims to replace human interventions with systems based on artificial intelligence. In this context, the task of detecting biofouling in monitoring images has been assigned to such systems. Artificial intelligence has advanced toward machine learning, with sophisticated techniques being developed for biofouling detection [1]. Early approaches used traditional machine learning algorithms, such as support vector machines and random forests, which were trained on handcrafted features extracted from images of marine structures. While these methods showed promise,

they were limited by their reliance on feature engineering and the need for extensive domain knowledge. The integration of deep learning into biofouling detection has significantly improved the accuracy and efficiency of these systems. CNNs have been particularly effective in automatically learning relevant features from large datasets, reducing the need for manual feature extraction. This is due to their architecture, which mainly consists of convolution and pooling layers for extracting features from input images, followed by fully connected layers to learn from these extracted features. Designing CNNs requires significant computational resources, allowing for the fine-tuning of parameters, and the training data play a crucial role in this process due to the large number of trainable parameters. To address these challenges, transfer learning has been introduced, allowing researchers to adapt pre-trained networks (e.g., AlexNet, SqueezeNet, ResNet) for more specific tasks, often requiring less data and computational effort [22].

While these networks are typically used for image classification, where the entire image is labeled with a single class, object detection requires a different approach. In object detection, an image may contain multiple objects, each with its own bounding box and class label. This means the network not only needs to classify objects but also needs to localize them within the image. For this reason, object detection networks must optimize three different aspects: box localization, box confidence, and classification [26].

One of the most popular object detection networks is YOLO (You Only Look Once), which has evolved significantly since its introduction in 2016. Unlike traditional classification networks, YOLO networks are designed to detect multiple objects in an image in real time, optimizing both speed and accuracy. Over the years, from YOLOv1 to YOLOv8, the architecture has improved in terms of object localization, multi-scale detection, and overall detection efficiency, making it one of the most effective approaches for real-time object detection tasks [27].

2.3. Biofouling Detection in Tidal Stream Turbines

Biofouling can significantly reduce the efficiency of these turbines by increasing drag and altering hydrodynamic performance, making early detection and management crucial for maintaining optimal performance [28,29]. Recent research has focused on applying deep learning-based detection algorithms to monitor biofouling on TSTs [30–32]. Mo et al. [32] presented a deep learning-based approach for identifying pollutant adhesion on tidal turbine blades. This method utilized a dataset of underwater images of turbines subjected to varying levels of artificial biofouling. By employing three different deep learning algorithms, the study enhanced the quality of biofouling images and applied image segmentation techniques to accurately extract and identify the location and extent of biofouling. The results demonstrated that this approach significantly improved the accuracy of biofouling detection, offering an efficient tool for the operation and maintenance of TSTs. Chen et al. [33] developed a semi-supervised video segmentation network (SVSN) for recognizing marine attachments on TST blades. To address the challenge of limited labeled data, their approach employs a data augmentation algorithm to generate sufficient labeled images from a smaller set of manually annotated frames. The SVSN utilizes a modified SegNet as the generator and a fully convolutional network as the discriminator, applying semi-supervised adversarial learning to integrate both labeled and unlabeled data. This methodology enhances the model's segmentation accuracy and generalization capabilities. The results demonstrate that the SVSN effectively identifies attachments and estimates uncertainties in harsh underwater conditions, offering a promising solution for maintaining TST efficiency. The issue of biofouling in TSTs using a soft-voting ensemble transfer learning approach for detection and classification is discussed by authors in [34]. The study introduced a comprehensive methodology that integrates data augmentation and preprocessing techniques, such as image resizing and segmentation, to handle biofouling challenges effectively. The authors acquired two datasets—one from Shanghai Maritime University (SMU) and another from Lehigh University (LU)—to train three prominent CNN models: Visual Geometry Group (VGG), Residual Network (ResNet), and MobileNet.

Their approach achieved notable accuracy rates of 0.83 for the SMU dataset and 0.90 for the LU dataset. The discrepancy in accuracy is attributed to the smaller size of the SMU dataset. The research highlights the importance of dataset scale in classification performance and provides valuable insights into improving biofouling detection and classification for TST systems.

In addition to image-based methods, Xu et al. [35] proposed a confidence-guided Dempster–Shafer (CDS) method for diagnosing turbine blade faults under the challenging conditions of swell effects and turbid water. This method combines stator current signals with image data, adapting to the confidence levels of each to improve the accuracy of fault diagnosis. The CDS method successfully addresses the limitations of single-sensor approaches, enhancing diagnostic performance even in complex underwater environments.

In conclusion, integrating deep learning-based object detection and fault diagnosis methods, particularly those employing models like YOLO, has significantly advanced the field of biofouling detection for TSTs. These technologies improve the efficiency and accuracy of monitoring systems and contribute to the sustainable operation of marine energy technologies by enabling proactive maintenance strategies.

3. Necessary Background

3.1. Biofouling in Images

The marine environment is home to a vast diversity of species, including fish, plants, algae, etc. Among these living organisms, biofouling stands out as the accumulation of marine organisms on submerged surfaces, which alters their texture. This phenomenon is particularly challenging to detect due to its rapid evolution in size and color, as well as its ability to blend into the surroundings [1]. Despite advances in camera technology and detection algorithms, these characteristics make biofouling detection a significant challenge, highlighting the need to develop methods better suited to this complex environment.

Such a problem can be associated with different computer vision tasks: classification, segmentation, and object detection [26]. Unlike the first two, object detection allows for the identification of multiple objects in a single image, something that classification cannot achieve. For example, if a camera is focused on a structure containing four turbines that need to be monitored, object detection provides a broader view by detecting objects within bounding boxes rather than analyzing every pixel as in segmentation. This approach makes it possible to monitor specific objects rather than the whole structure. This is particularly important, as the attachment of biological fouling to a fixed structure is less of a concern than on rotating objects such as blades.

3.2. YOLO

YOLOv8 is the latest version of object detection neural networks from Ultralytics, released in January 2023 by Jocher et al. [36], based on a CNN architecture, as described in [27]. The strength of this version lies in its integration of advanced feature extraction mechanisms, namely Cross Stage Partial (CSP) with a Darknet53 backbone, along with Spatial Pyramid Pooling (SPP). The combination of these two mechanisms enhances the model's ability to detect objects of various sizes and scales with high accuracy. Each image processed by YOLOv8 is associated with a tensor of dimensions $S \times S \times (B \times 5 + C)$, where S represents the number of grid cells, B refers to the bounding boxes containing five attributes (center coordinates x and y, width, height, and confidence), and C corresponds to the class annotations. The YOLO algorithm, in general, is optimized using three objective functions: Box Loss, Object Loss, and Class Loss (Equation (1)). The Box Loss function is responsible for adjusting the bounding boxes (Equation (2)). It aims to optimize the drawing of a box around an object based on the position of its center (x and y coordinates) as well as its dimensions (width and height). This function minimizes the localization error between the manually drawn box (ground truth) and the one predicted by the network, taking these geometric parameters into account. The Object Loss function handles object detection within the localized box (Equation (3)). It evaluates the probability of the presence or

absence of an object in the detected box, minimizing the error associated with this binary detection. Finally, the Class Loss function is involved in the classification of the detected object (Equation (4)). It is a classification operation that minimizes the error between the object class assigned in the training images and the one predicted by the network. This error is measured in terms of recognition probability, thus refining the model's ability to correctly classify objects. The mathematical formulation of this optimization problem is as follows [27]:

$$\text{YOLO cost function} = \text{Localization loss} + \text{Confidence loss} + \text{Classification loss} \quad (1)$$

Each of these sub-functions is designed to optimize a specific aspect of the object detection process, and formulated as bellow:

$$\begin{aligned}\text{Localization loss} =& \lambda_{coord} \sum_{i=0}^{S^2} \sum_{j=0}^{B} 1_{ij}^{obj} \left[(x_i - \hat{x}_i)^2 + (y_i - \hat{y}_i)^2 \right] \\ &+ \lambda_{coord} \sum_{i=0}^{S^2} \sum_{j=0}^{B} 1_{ij}^{obj} \left[\left(\sqrt{\omega_i} - \sqrt{\hat{\omega}_i} \right)^2 + \left(\sqrt{h_i} - \sqrt{\hat{h}_i} \right)^2 \right]\end{aligned} \quad (2)$$

$$\begin{aligned}\text{Confidence loss} =& \sum_{i=0}^{S^2} \sum_{j=0}^{B} 1_{ij}^{obj} \left[\left(C_i - \hat{C}_i \right)^2 \right] \\ &+ \lambda_{coord} \sum_{i=0}^{S^2} \sum_{j=0}^{B} 1_{ij}^{obj} \left[\left(C_i - \hat{C}_i \right)^2 \right]\end{aligned} \quad (3)$$

$$\text{Classification loss} = \sum_{i=0}^{S^2} 1_{ij}^{obj} \sum_{c \in classes} \left[\left(p_i(c) - \hat{p}_i(c) \right)^2 \right] \quad (4)$$

where λ_{coord} is a scale factor, i and j, for each grid box, x_i and y_i are coordinates in the ith cell, ω and h are coordinates in the ith cell, C_i is the confidence score, p_i is the probability of class c, and, with a caret for predicted values, 1_{ij}^{obj} is defined as 1 if the object appears and 0 otherwise.

3.3. Evaluation Metrics

Several metrics are employed to evaluate the quality of object detection using statistical criteria. The possible outcomes include true positives (TP), where the object is correctly detected; false positives (FP), where an object is detected but not actually present; false negatives (FN), where the object is present but not detected; and true negatives (TN), where no object is detected and none is present. These outcomes contribute to general evaluation metrics like accuracy and confusion matrices, as well as specific evaluation criteria for each class, which can be formulated as follows [37]:

$$Precision = \frac{TP + TN}{TP + TN + FP + FN} \quad (5)$$

$$Recall = \frac{TP}{TP + TN} \quad (6)$$

Based on these two metrics, mean average precision (mAP) is calculated as follows:

$$mAP = \sum_{k=1}^{N} P(k) \cdot \Delta r(k) \quad (7)$$

where k represents the number of recognized figures with precision (P) and recall gradient ($\Delta r(k)$).

4. Proposed Methodology

4.1. Dataset Presentation

Professor Yusaku Kyojuka from the Faculty of Engineering Sciences at Kyushu University in Japan designed a structure equipped with four turbines, each containing three blades spaced at 60 degrees to the axis of rotation, as shown in Figures 2 and 3. The structure was submerged on the seafloor next to the pier of Ikitsuki Bridge in Nagasaki, Hirado, and Kasugacho, Japan, at a depth of 7 m. The monitoring of biofouling attachment was carried out by a camera over 8 months, from August 2012 to April 2013 [38].

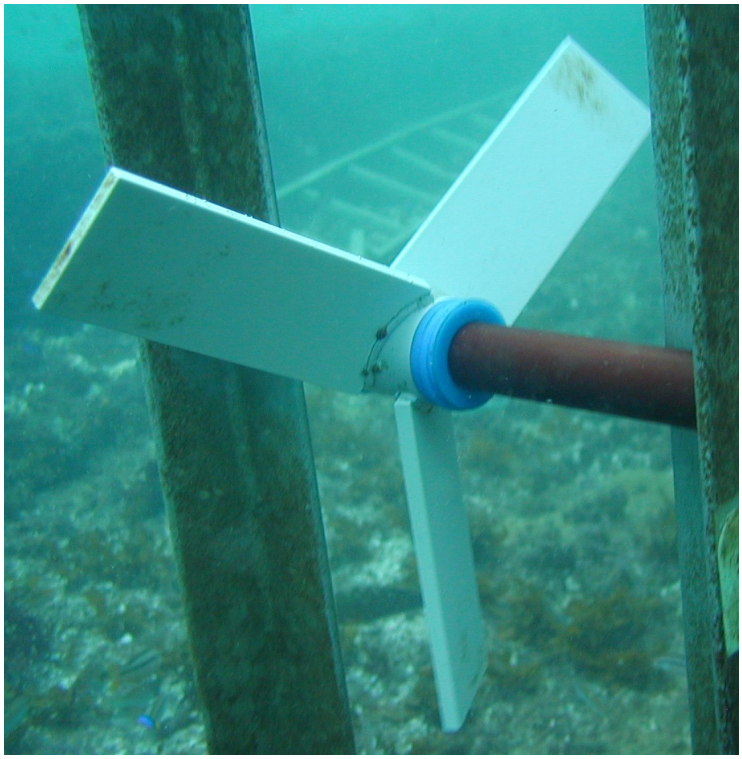

Figure 2. Tidal stream turbine blades structure.

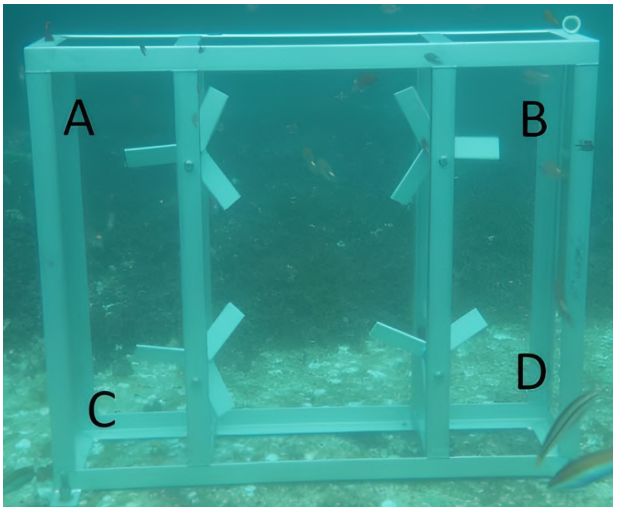

Figure 3. Submerged tidal stream turbine structure (four turbines (A–D)). Courtesy of Prof. Yusaku Kyozuka [39].

The dataset used in this study was obtained from two recorded videos of the four installed turbines. Each video had a duration of 15 s, with a frame rate of 60 frames per

second (fps), each video consisted of a total of 900 frames (15 s × 60 fps). This high frame rate provided a detailed view of the biofouling process, allowing for a thorough analysis of how biofouling developed on the turbine blades over time. The videos were captured at a resolution of 320 × 240 pixels with a data rate of 2600 Kbits/s using a CMOS sensor with progressive scan technology, ensuring that each frame is fully captured without interlacing artifacts. The videos were recorded on 20 October 2012, providing a clear and detailed view of how biofouling has developed on the turbine blades over time.

4.2. Proposed Model Evaluation

The methodology proposed in this paper, illustrated by the flowchart in Figure 4, uses images extracted from monitoring sequences of the four turbines described above, which are mounted on a submerged structure. The obtained images are labeled using a graphical image annotation tool named *labelImg.exe*, which is used to draw bounding boxes around objects in the images and label them with the appropriate class names. These labels are then prescribed in a file containing each box's boundaries and the corresponding class. In our case, the boxes are drawn around fouled and clean turbines, and each one is annotated accordingly.

The obtained images, along with their descriptive files, are divided into training and testing datasets, which are then used to train and evaluate the network. Due to a lack of data and relatively low accuracy, we opted for data augmentation to create a more effective model trained on noisier data, aiming to improve its accuracy. For this purpose, we used the latest official version of the YOLO series, YOLOv8 (version 8). Training the network involves defining specific training parameters, which are listed in Table 1 and obtained through random trial and error. The training process focuses on optimizing the three loss functions described earlier.

Table 1. Training options.

Options	Value
Optimizer	SGD
Learning rate	0.01
Mini batch size	16
Epochs	25
Test confidence threshold	0.25

To evaluate the training stage, we used unseen test images. The result of this stage includes the same test images with annotated boxes indicating the detection and its precision. The possible cases of false detection after testing are the following:

- Fouled turbines detected as clean.
- Clean turbines detected as fouled.
- Background detected as either clean or fouled.

The evaluation criteria included precision, recall, and mAP50 for the specific evaluation of each class, as well as the confusion matrix and accuracy for the overall evaluation. These criteria were calculated based on the confidence level of each detected object.
Sample images with detection boxes are provided to visually demonstrate the detection performance (Figure 5). The overall evaluation achieved an accuracy of 97.3%, as illustrated by the confusion matrix in Figure 6. The specific evaluation metrics for each class are detailed in Table 2.

Table 2. Evaluation metrics.

Class	Precision	Recall	mAP50	mAP50-95
Fouled	0.993	1.0	0.995	0.792
Clean	1.0	0.982	0.995	0.827

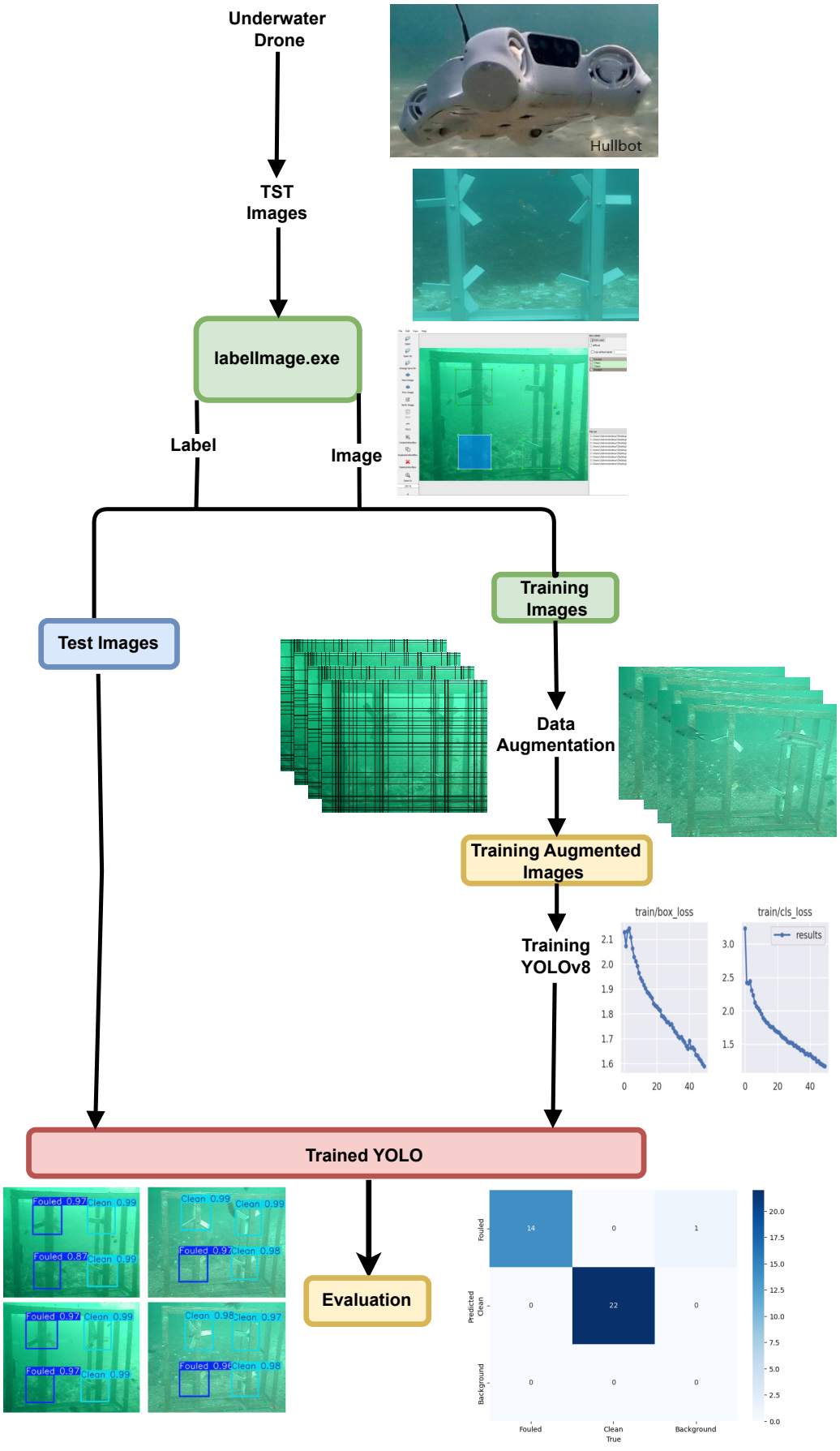

Figure 4. Proposed methodology flowchart.

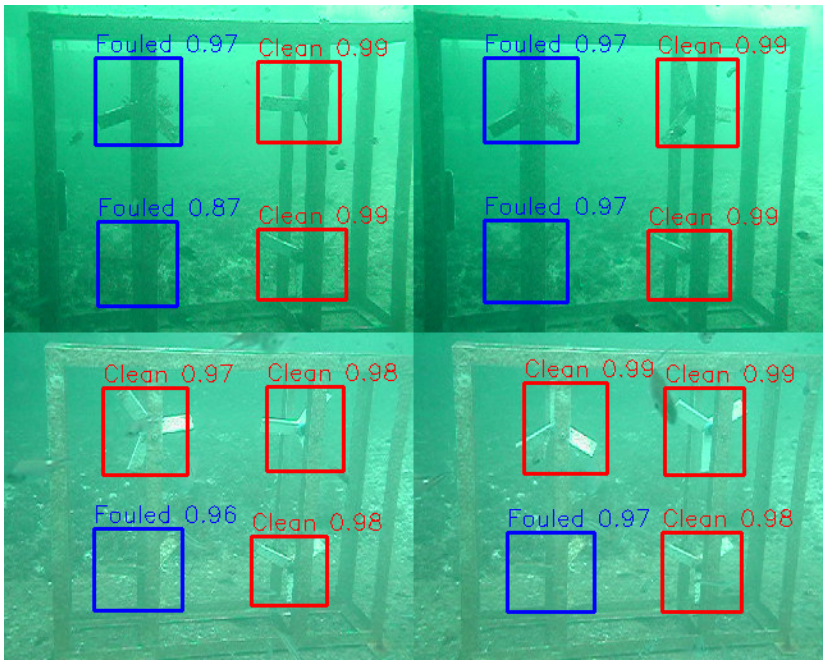

Figure 5. Detection samples.

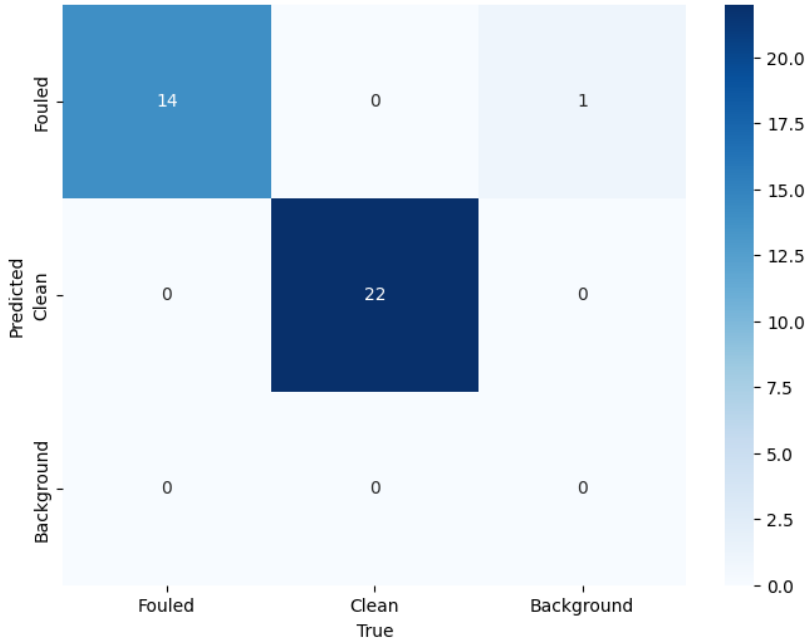

Figure 6. Confusion matrix.

The results obtained from object detection based on YOLOv8 demonstrate its effectiveness for detecting biofouling in a noisy environment containing other species, as shown in Figure 5.

4.3. Proposed Model Comparison

To demonstrate the usefulness of this object detection network for biofouling detection, a comparison was made between YOLOv8 and earlier versions (v3 and v5) with the same training settings (Table 1). The comparison includes the specific criteria shown in Table 3.

Table 3. Comparison metrics.

	Metric	Fouled	Clean
YOLOv3	Precision	1.0	0.656
	Recall	0.577	0.972
	mAP50	0.948	0.907
	mAP50-95	0.524	0.510
YOLOv5	Precision	0.444	0.1
	Recall	0.286	1.0
	mAP50	0.397	0.385
	mAP50-95	0.186	0.13
YOLOv8	Precision	0.993	1.0
	Recall	1.0	0.982
	mAP50	0.995	0.995
	mAP50-95	0.792	0.827

As anticipated, YOLOv8 emerges as the most effective model, demonstrating superior overall results in terms of precision, recall, mAP50, and mAP50-95, as shown in Table 3. YOLOv8 achieves nearly perfect precision for both the "Fouled" and "Clean" classes and maintains a high recall rate, reflecting its excellent overall performance. YOLOv3 performs well but falls short compared to YOLOv8, while YOLOv5 shows significantly lower scores across these metrics. Notably, YOLOv5 fails to detect any "Fouled" cases, as evidenced by zero true positives for this class, highlighting major limitations in its detection capabilities. In contrast, YOLOv3 does manage some detections, although its performance in this respect remains inferior to that of YOLOv8.

Additionally,YOLOv5 displays multiple detections for the same object with varying confidence levels, which can lead to information overload and inaccuracies in object labeling. YOLOv3 and YOLOv8 handle unique detections more effectively. YOLOv3 excels in background detection, indicating better handling of non-relevant scenes, while YOLOv5 is next in this aspect, with YOLOv8 being the least effective in background detection but excelling in detecting the objects of interest. YOLOv8 consistently maintains a confidence level above 0.85 for true positive detections, a notable improvement over the other models. The differences in performance among YOLOv3, YOLOv5, and YOLOv8 can be attributed to advancements in model architecture, training algorithms, and regularization techniques. YOLOv8's recent advancements provide a significant edge in precision and robustness. YOLOv3's high precision for "Fouled" but low recall suggests a conservative prediction approach, leading to missed detections. In contrast, YOLOv5's high recall for "Clean" but low precision indicates it detects almost everything as "Clean", often inaccurately. YOLOv8's balanced performance across precision and recall makes it the most comprehensive and effective model for object detection tasks.

4.4. Data Augmentation

Deep neural networks are highly effective for tasks such as detection and classification but typically require large amounts of training data to achieve accurate results. In the context of biofouling detection, obtaining an extensive dataset, particularly of faulty or fouled states, can be challenging due to the limited availability of such real-world conditions. To mitigate this issue, data augmentation techniques are employed to artificially expand the dataset by generating variations of the existing images, thereby enhancing the model's ability to generalize.

The augmentation techniques used in this study involve introducing structured noise into the images by randomly adding 10% of lines and columns. This method adds black lines to a subset of the rows and columns within the image, as illustrated in Figure 7. The 10% of lines and columns are selected at random for each image, ensuring that the noise pattern varies across the dataset [40].

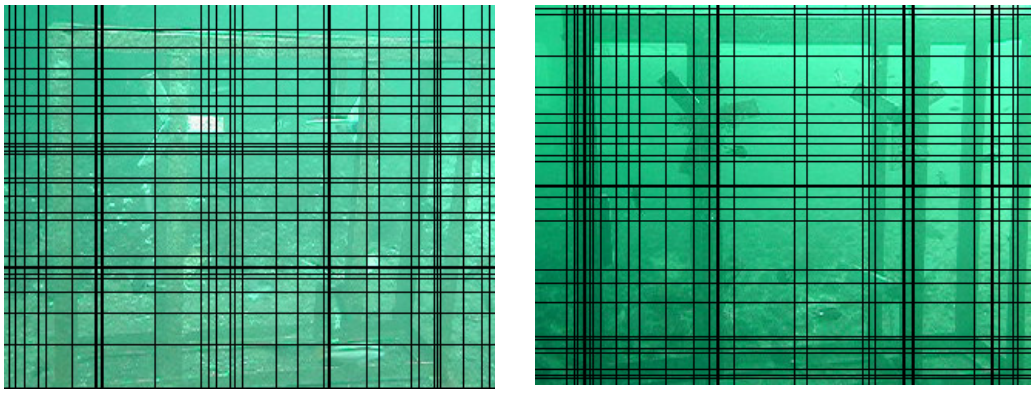

Figure 7. Data augmentation samples.

This augmentation simulates imperfections or artifacts that could naturally occur in real-world video sequences, such as those caused by environmental factors, sensor noise, or transmission errors. The added noise provides the model with examples of degraded or imperfect visual data, helping it become more robust in detecting biofouling even when the quality of the footage is compromised.

Furthermore, this process is applied uniformly across both the horizontal and vertical axes, ensuring that the spatial structure of the image is maintained, and the underlying features of the biofouling (e.g., edges, texture) remain recognizable to the neural network. Despite the introduction of noise, the essential characteristics of the image are preserved, and the augmentation technique does not alter the annotated regions of interest. This means the annotation boxes for the biofouling areas remain intact, ensuring that the model still learns from the correct labels.

The impact of data augmentation is in line with expectations, improving accuracy for all learning networks, including the different versions of YOLO in our case. Several points can be highlighted in Table 4. First, the evolution of the various metrics (precision, recall, mAP50, and mAP50-95) shows a similar trend, indicating that data augmentation positively affected both classes (clean and fouled). Second, the improvement was most significant for YOLOv5, followed by YOLOv3, and finally YOLOv8, reflecting the order from least to most accurate; hence, the effect of augmentation is more pronounced for the weaker model. Third, the superiority of YOLOv8 is clear both before and after augmentation, justifying its effectiveness for biofouling detection.

Table 4. Metric comparison, before and after data augmentation.

	Class	**Clean**	**Fouled**	**Clean**	**Fouled**
		Before Augmentation		**After Augmentation**	
YOLOv3	Precision	1.0	0.656	1.0	0.995
	Recall	0.577	0.972	1.0	1.0
	mAP50	0.948	0.907	0.995	0.995
	mAP50-95	0.524	0.510	0.749	0.733
YOLOv5	Precision	0.444	0.1	0.755	0.616
	Recall	0.286	1.0	0.714	1.0
	mAP50	0.397	0.385	0.868	0.581
	mAP50-95	0.186	0.130	0.581	0.483
YOLOv8	Precision	0.993	1.0	0.995	0.987
	Recall	1.0	0.982	1.0	1.0
	mAP50	0.995	0.995	0.995	0.995
	mAP50-95	0.792	0.827	0.814	0.837

5. Conclusions

This study demonstrates the potential of utilizing a camera-based surveillance system combined with YOLO 8 version models for biofouling detection. By converting video footage into annotated images and training the YOLO model, the system proved effective in distinguishing between biofouled and clean turbines. The results highlight YOLO version 8's superior performance over its predecessors, particularly when enhanced by a data augmentation approach. This not only improved detection accuracy but also addressed the issue of misdetection. The findings suggest that the automated detection of biofouling through advanced machine learning models like YOLO can significantly reduce the labor and costs associated with traditional methods, offering a promising solution for more efficient monitoring in marine industries.

Author Contributions: Conceptualization, H.R., H.H. and M.B.; methodology, H.R., H.H., Y.A. and M.B.; formal analysis, H.R., H.H., Y.A., A.M., H.T.-B. and M.B.; investigation, H.R. and H.H.; supervision, Y.A., A.M. and M.B.; writing—original draft preparation, H.R. and H.H. All authors have read and agreed to the published version of the manuscript.

Funding: This work is supported by the PIA 3 CMQ Industries de la Mer Bretagne (IndMer), France.

Institutional Review Board Statement: Not applicable.

Informed Consent Statement: Not applicable.

Data Availability Statement: Data available on request.

Acknowledgments: The authors would like to thank Yusaku KYOZUKA of Faculty of Engineering Sciences, Kyushu University for providing the dataset used in this study.

Conflicts of Interest: The authors declare no conflicts of interest.

References

1. Rashid, H.; Benbouzid, M.; Titah-Benbouzid, H.; Amirat, Y.; Mamoune, A. Tidal stream turbine biofouling detection and estimation: A review-based roadmap. *J. Mar. Sci. Eng.* **2023**, *11*, 908. [CrossRef]
2. Hopkins, G.; Davidson, I.; Georgiades, E.; Floerl, O.; Morrisey, D.; Cahill, P. Managing biofouling on submerged static artificial structures in the marine environment–Assessment of current and emerging approaches. *Front. Marine Sci.* **2021**, *8*, 759194. [CrossRef]
3. Thanthirige, T.R.M.; Goggins, J.; Flanagan, M.; Finnegan, W. A state-of-the-art review of structural testing of tidal turbine blades. *Energies* **2023**, *16*, 4061. [CrossRef]
4. Titah-Benbouzid, H.; Benbouzid, M.E.H. Biofouling issue on marine renewable energy converters: A state of the art review on impacts and prevention. *Int. J. Energy Convers.* **2017**, *5*, 67–78. [CrossRef]
5. Huisman, K.T.; Blankert, B.; Horn, H.; Wagner, M.; Vrouwenvelder, J.S.; Bucs, S.; Fortunato, L. Noninvasive monitoring of fouling in membrane processes by optical coherence tomography: A review. *J. Membr. Sci.* **2023**, *692*, 122291. [CrossRef]
6. Rashid, H.; Benbouzid, M.; Titah-Benbouzid, H.; Amirat, Y.; Berghout, T.; Mamoune, A. Mapping a Machine Learning Path Forward for Tidal Stream Turbines Biofouling Detection and Estimation. In Proceedings of the IECON 2023-49th Annual Conference of the IEEE Industrial Electronics Society, Singapore, 16–19 October 2023; pp. 1–6. [CrossRef]
7. Ancha, V.K.; Sibai, F.N.; Gonuguntla, V.; Vaddi, R. Utilizing YOLO Models for Real-World Scenarios: Assessing Novel Mixed Defect Detection Dataset in PCBs. *IEEE Access* **2024**, *12*, 100983–100990. [CrossRef]
8. Chen, X.; Yuan, M.; Yang, Q.; Yao, H.; Wang, H. Underwater-YCC: Underwater target detection optimization algorithm based on YOLOv7. *J. Mar. Sci. Eng.* **2023**, *11*, 995. [CrossRef]
9. Zhang, N.; Yang, G.; Wang, D.; Hu, F.; Yu, H.; Fan, J. A Defect Detection Method for Substation Equipment Based on Image Data Generation and Deep Learning. *IEEE Access* **2024**, *12*, 105042–105054. [CrossRef]
10. Zhao, Z.; Zheng, P.; Xu, S.; Wu, X. Object detection with deep learning: A review. *IEEE Trans. Neural Netw. Learn. Syst.* **2019**, *30*, 3212–3232. [CrossRef]
11. Zou, Z.; Chen, K.; Shi, Z.; Guo, Y.; Ye, J. Object detection in 20 years: A survey. *Proc. IEEE* **2023**, *111*, 257–276. [CrossRef]
12. Wang, Y.-Q. An analysis of the Viola-Jones face detection algorithm. *Image Process. Line* **2014**, *4*,128–148. [CrossRef]
13. Lei, J.; Luo, X.; Fang, L.; Wang, M.; Gu, Y. Region-enhanced convolutional neural network for object detection in remote sensing images. *IEEE Trans. Geosci. Remote Sens.* **2020**, *58*, 5693–5702. [CrossRef]
14. Xu, X.; Zhao, M.; Shi, P.; Ren, R.; He, X.; Wei, X.; Yang, H. Crack detection and comparison study based on faster R-CNN and mask R-CNN. *Sensors* **2022**, *22*, 1215. [CrossRef]

15. Magalhães, S.A.; Castro, L.; Moreira, G.; Santos, F.N.D.; Cunha, M.; Dias, J.; Moreira, A.P. Evaluating the single-shot multibox detector and YOLO deep learning models for the detection of tomatoes in a greenhouse. *Sensors* **2021**, *21*, 3569. [CrossRef] [PubMed]
16. Niu, S.; Xu, X.; Liang, A.; Yun, Y.; Li, L.; Hao, F.; Bai, J.; Ma, D. Research on a lightweight method for maize seed quality detection based on improved YOLOv8. *IEEE Access* **2024**, *12*, 32927–32937. [CrossRef]
17. Qin, X.; Yu, C.; Liu, B.; Zhang, Z. YOLO8-FASG: A high-accuracy fish identification method for underwater robotic system. *IEEE Access* **2024**, *12*, 73354–73362. [CrossRef]
18. Gai, R.; Liu, Y.; Xu, G. TL-YOLOv8: A blueberry fruit detection algorithm based on improved YOLOv8 and transfer learning. *IEEE Access* **2024**, *12*, 86378–86390. [CrossRef]
19. Diwan, T.; G, A.; Tembhurne, J.V. Object detection using YOLO: Challenges, architectural successors, datasets and applications. *Multimed. Tools Appl.* **2023**, *82*, 9243–9275. [CrossRef]
20. Ragab, M.G.; Abdulkader, S.J.; Muneer, A.; Alqushaibi, A.; Sumiea, E.H.; Qureshi, R.; Al-Selwi, S.M.; Alhussian, H. A comprehensive systematic review of YOLO for medical object detection (2018 to 2023). *IEEE Access* **2024**, *12*, 57815–57836. [CrossRef]
21. Liu, Y.; An, D.; Ren, Y.; Zhao, J.; Zhang, C.; Cheng, J.; Liu, J.; Wei, Y. DP-FishNet: Dual-path pyramid vision transformer-based underwater fish detection network. *Expert Syst. Appl.* **2024**, *238*, 122018. [CrossRef]
22. Habbouche, H.; Rashid, H.; Amirat, Y.; Banerjee, A.; Benbouzid, M. A 2D VMD video image processing-based transfer learning approach for the detection and estimation of biofouling in tidal stream turbines. *Ocean Eng.* **2024**, *312*, 119283. [CrossRef]
23. Xia, Z.; Gu, J.; Wen, Y.; Cao, X.; Gao, Y.; Li, S.; Haffner, G.D.; MacIsaac, H.J.; Zhan, A. eDNA-based detection reveals invasion risks of a biofouling bivalve in the world's largest water diversion project. *Ecol. Appl.* **2024**, *34*, e2826. [CrossRef] [PubMed]
24. Cesaria, M.; Alfinito, E.; Arima, V.; Bianco, M.; Cataldo, R. MEED: A novel robust contrast enhancement procedure yielding highly-convergent thresholding of biofilm images. *Comput. Biol. Med.* **2022**, *151*, 106217. [CrossRef] [PubMed]
25. Goodwin, M.; Halvorsen, K.T.; Jiao, L.; Knausgård, K.M.; Martin, A.H.; Moyano, M.; Oomen, R.A.; Rasmussen, J.H.; Sørdalen, T.K.; Thorbjørnsen, S.H. Unlocking the potential of deep learning for marine ecology: Overview, applications, and outlook. *ICES J. Mar. Sci.* **2022**, *79*, 319–336. [CrossRef]
26. Kaur, R.; Singh, S. A comprehensive review of object detection with deep learning. *Digit. Signal Process.* **2023**, *132*, 103812. [CrossRef]
27. Terven, J.; Córdova-Esparza, D.M.; Romero-González, J.A. A comprehensive review of YOLO architectures in computer vision: From YOLOv1 to YOLOv8 and YOLO-NAS. *Machine Learn. Knowl. Extr.* **2023**, *5*, 1680–1716. [CrossRef]
28. Zeng, X.; Shao, Y.; Feng, X.; Xu, K.; Jin, R.; Li, H. Nonlinear hydrodynamics of floating offshore wind turbines: A review. *Renew. Sustain. Energy Rev.* **2024**, *191*, 114092. [CrossRef]
29. Titah-Benbouzid, H.; Rashid, H.; Benbouzid, M. Biofouling issue in tidal stream turbines. In *Design, Control and Monitoring of Tidal Stream Turbine Systems*; IET: London, UK, 2023; pp. 181–204.
30. Song, D.; Liu, R.; Zhang, Z.; Yang, D.; Wang, T. IRNLGD: An Edge Detection Algorithm with Comprehensive Gradient Directions for Tidal Stream Turbine. *J. Mar. Sci. Eng.* **2024**, *12*, 498. [CrossRef]
31. Wang, L.; Xu, J.; Luo, W.; Luo, Z.; Xie, J.; Yuan, J.; Tan, A.C.C. A deep learning-based optimization framework of two-dimensional hydrofoils for tidal turbine rotor design. *Energy* **2022**, *253*, 124130. [CrossRef]
32. Mo, C.; Zhu, W.; Lu, B.; Zu, S.; Zhang, F.; Chen, J.; Zhang, X.; Wu, B.; Zhang, X.; Huang, J. Recognition method of turbine pollutant adhesion in tidal stream energy generation systems based on deep learning. *Energy* **2024**, *302*, 131799. [CrossRef]
33. Chen, L.; Peng, H.; Yang, D.; Wang, T. An attachment recognition method based on semi-supervised video segmentation for tidal stream turbines. *Ocean Eng.* **2024**, *293*, 116466. [CrossRef]
34. Rashid, H.; Benbouzid, M.; Amirat, Y.; Berghout, T.; Titah-Benbouzid, H.; Mamoune, A. Biofouling detection and classification in tidal stream turbines through soft voting ensemble transfer learning of video images. *Eng. Appl. Artif. Intell.* **2024**, *138*, 109316. [CrossRef]
35. Xu, Y.; Wang, T.; Diallo, D.; Amirat, Y. A confidence-guided DS fault diagnosis method for tidal stream turbines blade. *Ocean Eng.* **2024**, *311*, 118807. [CrossRef]
36. Jocher, G.; Chaurasia, A.; Qiu, J. *Ultralytics YOLO*, Version 8.0.0. 2023. Available online: https://github.com/ultralytics/ultralytics (accessed on 1 July 2024).
37. Xiao, Y.; Wang, X.; Zhang, P.; Meng, F.; Shao, F. Object detection based on faster R-CNN algorithm with skip pooling and fusion of contextual information. *Sensors* **2020**, *20*, 5490. [CrossRef] [PubMed]
38. Kyozuka, Y.; Ida, M.; Katsuyama, I.; Kobayashi, S.; Igawa, S. Study on marine biofouling effects on tidal power generator. In Proceedings of the 24th Ocean Engineering Symposium, Hiroshima, Japan, 3 March 2014; Volume 14, p. 2014. (In Japanese)
39. Katsuyama, I.; Kobayashi, S.; Igawa, S.; Kyozuka, Y.; Ida, M. Biofouling of model turbines for tidal current power generation and the effect of anti-fouling paint. *Sess. Org. (Sess. Org. Soc. Jpn.)* **2014**, *31*, 1–5. [CrossRef]
40. Habbouche, H.; Amirat, Y.; Benkedjouh, T.; Benbouzid, M. Bearing fault event-triggered diagnosis using a variational mode decomposition-based machine learning approach. *IEEE Trans. Energy Convers.* **2021**, *37*, 466–474. [CrossRef]